MNRAS 000, 1–?? (2016) Preprint 1 December 2016 Compiled using MNRAS LATEX style file v3.0

The spatial distribution of ultra diffuse galaxies within large scale structures

Javier Román[1,2] ⋆ and Ignacio Trujillo[1,2]
[1]Instituto de Astrofísica de Canarias, c/ Vía Láctea s/n, E-38205, La Laguna, Tenerife, Spain
[2]Departamento de Astrofísica, Universidad de La Laguna, E-38206, La Laguna, Tenerife, Spain

arXiv:1603.03494v2 [astro-ph.GA] 30 Nov 2016

ABSTRACT

Taking advantage of the SDSS Stripe82 data, we have explored the spatial distribution of ultra diffuse galaxies (UDGs) within an area of 8×8 Mpc^2 centered around the galaxy cluster Abell 168 (z=0.045). This intermediate massive cluster (σ=550 km/s) is surrounded by a complex large scale structure. Our work confirms the presence of UDGs in the cluster and in the large scale structure that surrounds it. Approximately 50% of the UDGs analysed inhabit the cluster region: ∼11±5% in the core and ∼39±9% in the outskirts whereas the remaining UDGs are found outside the main cluster structure ∼50±11%. UDGs structural properties gradually change from the lowest to the densest regions with a decrease of the stellar mass (by a factor of ∼1.5), a decrease of the radius (by a mean of 0.23 kpc), fainter average surface brightness, larger Sérsic index n and a lower axis ratio. This transformation supports the idea that UDGs form outside clusters and are later on accreted towards the central regions of the cluster, where they are destroyed by disruption. Finally, the spatial distribution of the UDGs is very similar to that found for dwarf galaxies but significantly different from the distribution of galaxies like the Milky Way, suggesting that UDGs could be bona fide dwarfs and not failed L$_\star$ galaxies.

Key words:
galaxies: evolution – galaxies: formation – galaxies: structure – galaxies: photometry – galaxies: dwarf

1 INTRODUCTION

Following pioneering work by Impey et al. (1988), Bothun et al. (1991) and Dalcanton et al. (1997), a number of recent works (e.g. van Dokkum et al. 2015; Koda et al. 2015; Mihos et al. 2015; van der Burg et al. 2016), using deep imaging of nearby clusters, have focused their attention on a type of low mass (10^7-10^8 M$_\odot$), low surface brightness (24<μ_g(0)<26 mag arcsec^{-2}) and extended size (1.5<r$_e$<4.5 kpc) galaxies. van Dokkum et al. (2015) have named these objects "ultra-diffuse galaxies" (UDGs). To date, UDGs have been found mostly in galaxy clusters. However, it is unclear whether this is just a bias produced by the strategy used to detect these objects. Due to their extreme low surface brightness, obtaining a spectroscopic redshift of these galaxies is very time consuming and their "redshifts" have been guessed by their proximity to a high density region. In fact, of the two UDGs confirmed spectroscopically (van Dokkum et al. 2015; Martínez-Delgado et al. 2016), one is in Coma and the other one is in a much lower density environment. Moreover, there are also known a small number of large, low surface brightness galaxies in the field (Dalcanton et al. 1997; Burkholder et al. 2001). Nonetheless, despite the observational bias towards galaxy clusters, the fact that the number of UDGs increases with cluster richness (van der Burg et al. 2016), with almost a doubling of the population of known galaxies in Coma (Koda et al. 2015) to barely adding a few candidates in Fornax (Muñoz et al. 2015), suggests that the environmental density could play a role in the origin of the UDGs.

From the theoretical point of view, Yozin & Bekki (2015) have shown that a scenario in which UDGs are satellites of a cluster, having infallen early at z∼2 and quenching their further growth, is able to reproduce the structural properties of these objects. Interestingly, one of the predictions of this scenario is that UDGs should not survive close to the centre of clusters as tides exerted by the cluster mass within that region will disrupt the infalling UDGs. This seems to be in agreement with the findings of van der Burg et al. (2016). For all the above reasons, it is clear that understanding in which environments UDGs are originally formed, i.e. whether they have been formed in-situ in the clusters or whether they have been accreted through infalling substructures (group, filaments) is fundamental to disentangle the origin of these mysterious galaxies. Another key feature to better understand the nature of the UDGs is to compare their spatial distribution with two different families of galaxies: dwarf versus L$_\star$. Among other scenarios, van Dokkum et al. (2015) discuss the intriguing possibility that UDGs are failed L$_\star$

⋆ E-mail:jroman@iac.es

© 2016 The Authors

galaxies. Other works have explored the possibility that UDGs are regular dwarf galaxies embedded in very massive dark matter halos (e.g. Beasley et al. 2016), dwarf galaxies inhabiting high-spin halos (Amorisco & Loeb 2016), failed LMC-like galaxies (Beasley & Trujillo 2016) or pure stellar halo galaxies (Peng & Lim 2016). Addressing which spatial distribution UDGs resemble most can shed extra light on the origin of these galaxies.

In this paper, we explore the distribution and properties of the population of UDGs inside and around the Abell 168 galaxy cluster (z=0.045). Abell 168 is a cluster with a richness II-III (BM classification) located at R.A.(2000)=01h15m12.0s and Dec (2000)=+00d19m48s. This cluster has a velocity dispersion of σ=550 km s^{-1} and a dynamical mass of M_{dyn}=5.2×10^{14} $M_{\odot}$ (Yang et al. 2004). The large scale structure surrounding this cluster is particularly relevant in order to probe where UDGs are born. In fact, around Abell 168 there are many filaments and galaxy groups, as well as a number of low density regions. Our large scale structure is fully embedded within the Sloan Digital Sky Survey (SDSS) Stripe 82. This means that we have deep photometry in 3 SDSS bands (g=25.2 mag, r=24.7 mag, i=24.3 mag; 3σ point sources), which implies having an extra filter compared to previous UDG works in other clusters. We will show that this extra filter is key to cleaning our galaxy sample from background contaminants. This will allow us to select UDGs candidates at the redshift of the cluster, but significantly further away from its center. To characterize in great detail the large scale structure around Abell 168, we use the deep spectroscopic coverage of this field produced by the SDSS survey in this area of the Stripe 82. In this paper, we explore a field of view of 2.5×2.5 degrees, equivalent to 8×8 Mpc around this cluster.

The structure of the paper is as follows. Section 2 describes the data. We explain how UDGs were identified in Section 3. The structural properties of the UDG sample is detailed in Section 4 and their spatial distribution is explored in Section 5. The analysis of the local environment effects on the structural and colour properties of the UDGs is described in Section 6. Section 7 address a potential link between UDGs and regular dwarf galaxies. Finally, Section 8 presents a discussion of the results whereas Section 9 summarize our main findings. Throughout this paper, we adopt the following cosmology Ω_m=0.3, Ω_Λ=0.7 and H_0=70 km s^{-1} Mpc^{-1}. The spatial scale is 0.885 kpc/″at the Abell 168 redshift (z=0.045). We use the AB-magnitude system in this work.

2 DATA

The images used in this paper were obtained from The IAC Stripe 82 Legacy Survey[1] (Fliri & Trujillo 2016). The IAC Stripe 82 Legacy Survey consists on a new deep co-adds of the Stripe 82 data from SDSS, especially stacked to reach the faintest surface brightness limits of this data set. The average surface brightness limit is r∼28.5 mag/arcsec^2 (3σ obtained in 10×10 arcsec boxes). The Stripe 82 covers a 2.5 degree wide region along the celestial equator (-50°< R.A. < 60 °, -1.25 °< Dec. < 1.25 °) with a total of 275 square degrees. The pixel scale of the imaging is 0.396″. This region of the sky has been imaged repeatedly approximately 80 times in all the five SDSS filters (u, g, r, i and z). The IAC project provides the imaging dataset in 0.5×0.5 degrees blocks. We created a final mosaic of 2.5×2.5 degrees using SWarp[2] (Bertin et al. 2002) centred approximately at the coordinates of the Abell 168 cluster (R.A.=18.8°, Dec.=0.33°). The limiting surface brightness of the entire region was measured in each 0.5×0.5 degrees block. We found that the surface brightness depth across the whole area is reasonably homogeneous, with a mean depth at the 3σ level (in 10×10 arcsec boxes) of 29.2, 28.7 and 28.2 mag arcsec^{-2} in the g, r and i filters respectively.

[1] http://www.iac.es/proyecto/stripe82/
[2] http://www.astromatic.net/software/swarp

3 IDENTIFICATION

The goal of this paper is to find UDGs inside and around Abell 168. With this aim, we ran SExtractor (Bertin & Arnouts 1996) on the entire mosaic in the above 3 filters, plus another filter provided by the IAC project "r-deep" which is the combination of g, r and i. As we are interested in the detection of extended sources with very low surface brightness, we use a detection threshold in all the bands of 1σ and a minimum area of 25 pixels (i.e. 4 arcsec^2 or 3 kpc^2 at the cluster redshift). With these settings, SExtractor found a total of 331891 sources in the r-deep filter. We further reduced our list of galaxies by requesting that the sources were identified in all the above bands. In addition, all the sources are selected to have simultaneously a stellarity (CLASS_STAR) below 0.15 in each filter (to avoid selecting point-like objects).

The next selection criteria is based on the photometric colour (MAG_AUTO) of the sources. We conservatively select the following ranges: 0<g-r<1.2, 0<g-i<1.7 and -0.2<r-i<0.7. These colour intervals are broader than the expected colour values for the galaxy population (red and blue) at the cluster redshift (as we will show later). After all these selection criteria we are left with 75666 galaxies.

The identification of UDGs requires a measurement of the size and surface brightness of the galaxies. For this reason, we ran on all the preselected galaxies the IMFIT code (Erwin 2015). We used a Sérsic model (Sersic 1968) to extract the structural parameters of our preselected galaxies. We provided as input parameters for IMFIT the coordinates of the source, position angle and effective radius retrieved from the SExtractor run. IMFIT ran over the g, r and i filters. For each individual fitting, we masked all the pixels of nearby sources detected by SExtractor. The Sérsic models were convolved with the PSF of the images. These PSFs are provided by the IAC Stripe 82 Legacy Survey for each individual block.

The structural parameters obtained from the Sérsic fit are: position angle, ellipticity, Sérsic index n, effective radius r_e and total magnitude in each filter. Up to three slightly different input parameters in each individual fitting have been tried to ensure robustness of the output structural parameters of IMFIT. In most cases, the difference between the IMFIT results is negligible, but to be consistent we use the mean values of these three outputs. We compare the magnitude and effective radius values from IMFIT and SExtractor as a quality check of the fitting process, and we obtain a very good correlation between both magnitudes and a reasonably good correlation for the effective radii (see Fig. A1 in the Appendix). The SExtractor effective radius value does not account for the PSF effect, so it is expected that these values will be slightly larger than those obtained by the IMFIT code, particularly for the most compact objects. Sources showing large magnitude differences (>1 mag) between IMFIT and SExtractor were flagged and visually inspected. These objects represent a tiny fraction of the total number of fitted sources (∼0.5% in g band). They are usually artifacts of the image, interacting galaxies, very bright galaxies with multiple

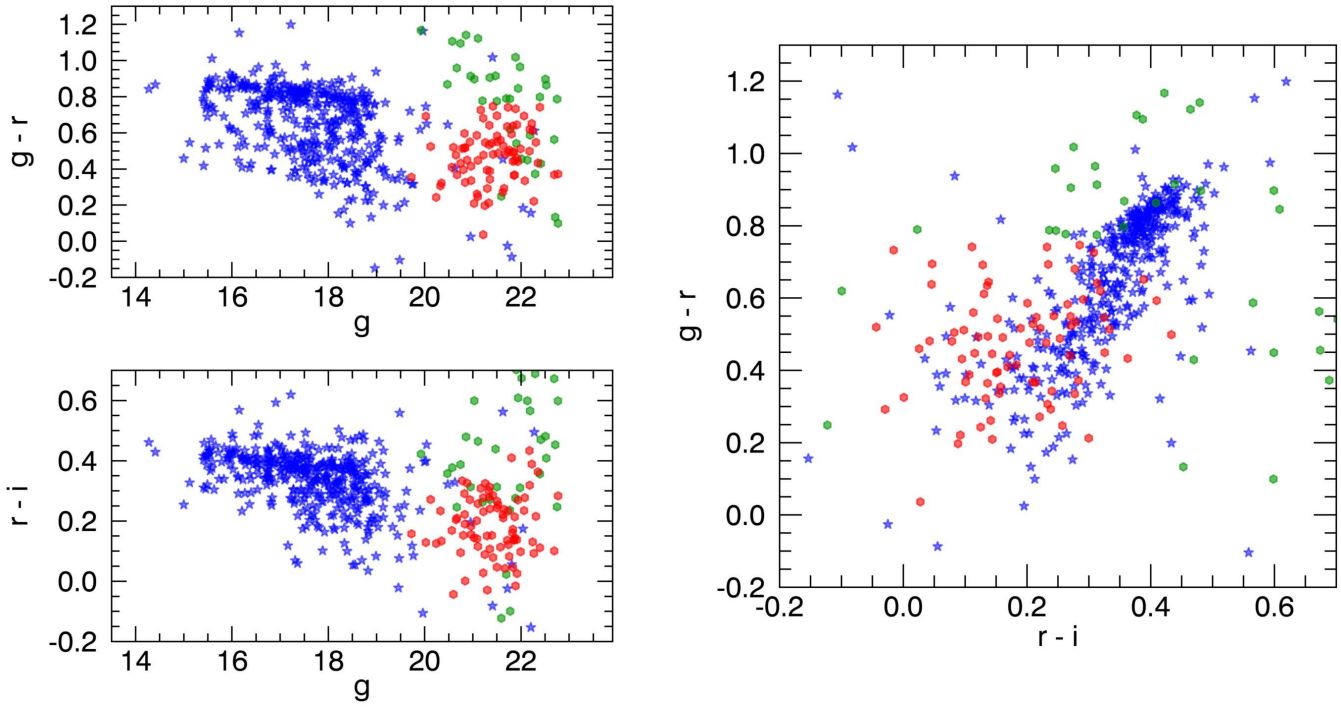

Figure 1. Colour magnitude and colour-colour maps of the galaxies in the field of view of Abell 168. The blue stars correspond to galaxies in the area of Abell 168 with spectroscopic redshifts 0.037<z<0.052. The red circles are the UDG candidates that have been selected as compatible with being at the cluster redshift using the colour distribution of the galaxies with spectroscopic redshifts. The green circles are those UDG candidates considered as potential contaminants due to their colours.

pieces detected by SExtractor, bad fits of the IMFIT code, etc. We do not further consider these objects in the analysis.

3.1 Selection of UDGs

Following previous works in the literature, the selection of UDGs in our field is based on the size and surface brightness of the galaxies. We use the structural parameters (magnitude, effective radius, n and ellipticity) provided by IMFIT to do our final cut. The magnitudes of the galaxies were corrected by the dust extinction of our Galaxy. Across our field of view, the dust extinction is relatively homogeneous and we select the following corrections: 0.098, 0.068 and 0.051 mag for the g, r and i filters respectively (Schlafly & Finkbeiner 2011). Due to the low redshift of our galaxies, z∼0.045, the K-corrections are very small, K_g ∼0.05, (see e.g. http://kcor.sai.msu.ru/; Chilingarian et al. 2010) and therefore we have not corrected our galaxies of this effect.

Assuming that UDGs are well described by an exponential light distribution, van Dokkum et al. (2015) use the following criteria to select them: $\mu_g(0)$ >24 mag/arcsec^2 and semimajor effective radius r_e >1.5 kpc. Koda et al. (2015), analyzing a large number of UDG candidates, show that their Sérsic index n distribution peaks towards slightly lower values than n=1 (see their Fig. 4). They also find that their axis ratio distribution has a broad shape with a maximum around 0.75. Based on that, we use the following criteria:

(i) $\mu_g(0)$>24.0 mag/arcsec^2 after correction by dust extinction. $\mu_g(0)$ is obtained using a Sérsic model with n free.

(ii) Circularized R_e>1.25 kpc. Taking into account the typical axis ratio measured for these objects, this is equivalent to selecting galaxies with semimajor effective radius $r_e \gtrsim$1.5 kpc.

After applying these criteria we get 124 UDG candidates. All these candidates were visually inspected in order to eliminate artifacts misclassified as real UDGs. Examples of incorrectly detected UDGs are groups of sources detected as a single object by SExtractor or mergers of galaxies. To visually discard some of these contaminants, we took advantage of colour stamps created by the combination of g, r and i filters. After this visual inspection we are left with 113 galaxies.

The next step is to select the UDGs that are at the distance of the Abell 168 structure and its surroundings. Lacking spectroscopic redshifts for our faint sources, the approach we have followed is to study the colour distribution of the galaxies with spectroscopic redshifts in the field compatible with being at the cluster redshift (i.e. z=0.045). In particular, we have selected all the galaxies with spectroscopic redshifts 0.037<z<0.052 (i.e. those compatible with being within 3σ the velocity distribution of the Abell 168 cluster and the observed redshift distribution around this peak in the redshift histogram). The colour-magnitude and colour-colour maps for these spectroscopic sources are presented in Fig. 1. The limiting apparent magnitude in this field for having spectroscopic redshift is g∼19 mag. Fig. 1 shows that galaxies with spectroscopic redshifts have a broad distribution in colour, ranging from red galaxies defining a clear red sequence to objects following a blue cloud. The individual error in magnitude for each of the sources is key to characterize the broadening of the colour distribution[3], particularly in the colour-colour maps. We have used the regular SDSS photomet-

[3] The magnitude uncertainty for each of our UDG candidates is σ_g=0.07 mag, σ_r=0.07 mag and σ_i=0.11 mag. These values are obtained comparing the magnitudes obtained in IMFIT versus SExtractor for galaxies in the range 20.5<g<22.5.

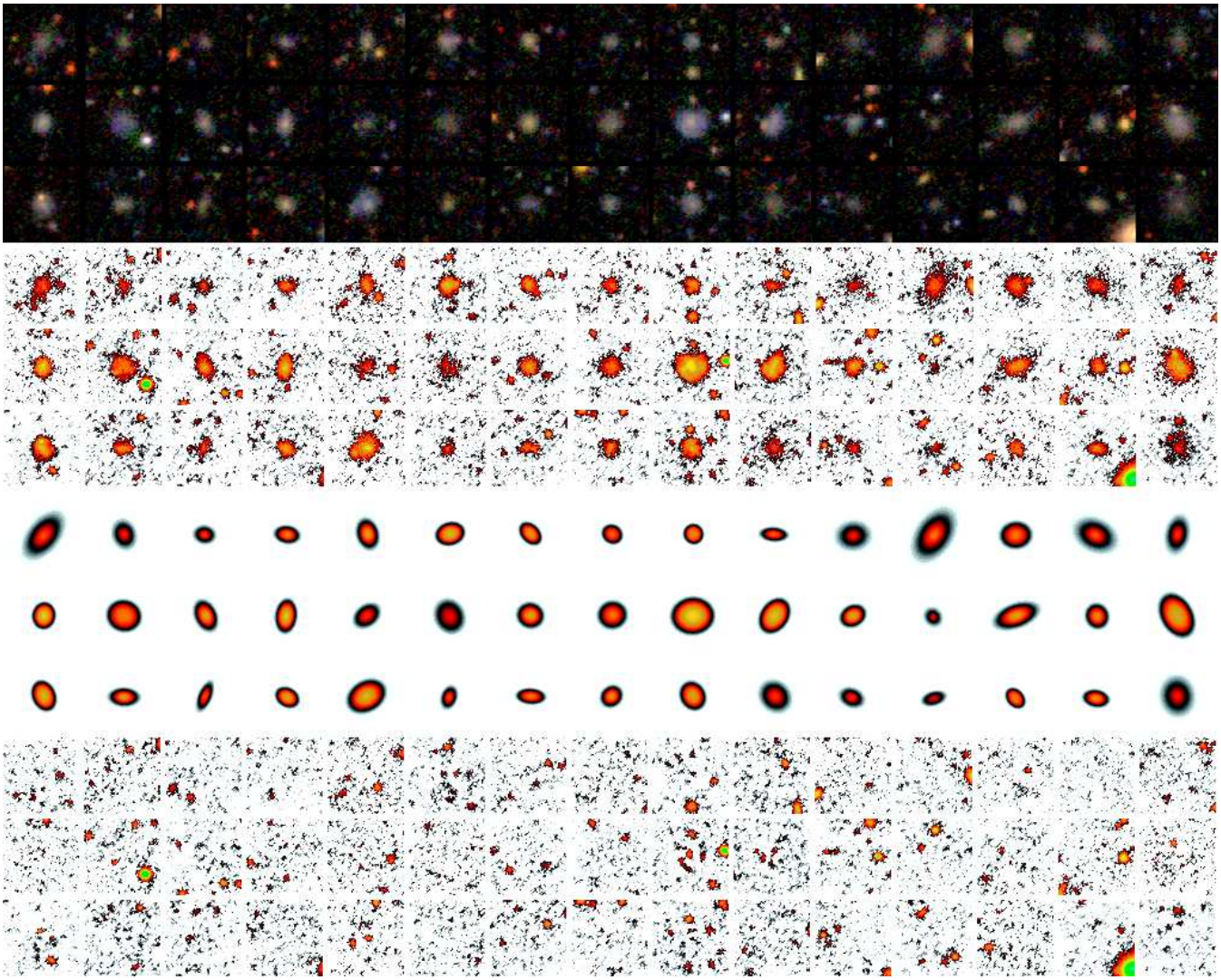

Figure 2. Mosaic showing a representative example of the UDGs explored in this paper. The colour stamps have been created using the filters g, r and i. The second row of images are the same galaxies in the g-band filter. The third row corresponds to the IMFIT model used to parameterize the galaxies. The last set of images are the residuals after subtracting the IMFIT models from the images.

ric data for our spectroscopic sources (this data is ∼2 mag shallower than Stripe 82). In doing this, we obtain (for the faintest galaxy with spectroscopic redshift) an uncertainty in the colour-colour map that is pretty close to the one we get for the ∼2 mag fainter UDGs using Stripe 82 data.

The final step is to separate galaxies compatible with having the same colour distribution as the spectroscopic sample. For this reason, our final UDG candidates must to share the same colour distribution of the spectroscopic sample in the colour-colour map shown in Fig. 1. To do this, we estimate the distance of each of our UDG candidates in the 2D colour space (g-r, r-i) to the third nearest galaxy with spectroscopy. We select the third nearest object to have a more robust estimation than just using the first. We require that the 3rd object not to be further away than 0.2 mag in this colour-colour plane. Additionally we restrict the colour of our UDGs to g-r<0.75 and r-i<0.45 trying to avoid background contaminants from distant red galaxies. Those UDGs satisfying this criterion are shown with red symbols, those with colours not compatible with the spectroscopic sample with green dots. Our final sample of UDGs compatible with being at the redshift of Abell 168 consists of 80 objects. A representative sample of these UDGs is shown in Fig. 2. There are 33 galaxies incompatible with being at the cluster distance. This implies a typical contamination level for surveys like ours that have not this extra colour of ∼30%. The average colours of the contaminant galaxies are: $< g - r >$=0.75 (r.m.s.=0.29) and $< r - i >$=0.40 (r.m.s.=0.21).

Despite the fact that we use a third filter to clean our sample of contaminants, it is clear that we still should have a level of contamination due to foreground and background objects. Not having spectroscopic redshifts it is difficult to estimate accurately the level of this remaining contamination. Our colour-colour, size and surface brightness selection criteria eliminate most of the background interlopers (at least those with z>0.1). We have explored in Section 5.1 how much of this contamination could still be in place using the vicinity of the UDG candidates to spectroscopic galaxies in the large scale structure of Abell 168 and the proximity to spectroscopic galaxies as a proxy.

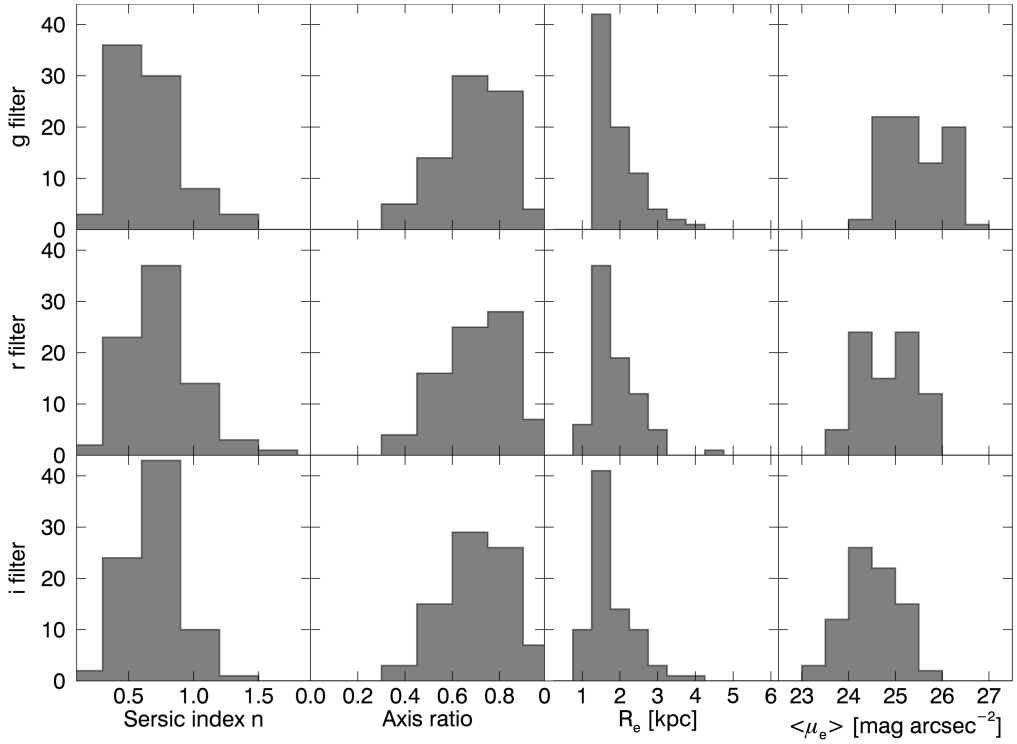

Figure 3. Distribution of structural parameters obtained using a Sérsic fit to the whole sample of UDGs in the g, r and i filters.

4 STRUCTURAL PROPERTIES OF THE UDG SAMPLE

Once the sample of UDGs compatible with being at the redshift of cluster Abell 168 is selected, we explore the distribution of their structural properties (see Table B1). This is shown in Fig. 3. We show in the figure, for each filter, the distribution of the Sérsic index n, the axis ratio, the circularized effective radius R_e and the average surface brightness within the effective radius $<\mu_e>$. The distribution of all the structural properties is quite similar in all the bands (see Fig. A2), except as expected for $<\mu_e>$ which changes due to the colours of the UDGs. As has been found in previous works (e.g. Koda et al. 2015; van der Burg et al. 2016) the Sérsic indexes n of the UDGs are slightly below 1, with a peak around 0.7 ($< n_g >$=0.65, $< n_r >$=0.74 and $< n_i >$=0.69). Interestingly, almost none of the UDGs has n >1.5. Also, the axis ratio of these objects is around 0.7, suggesting an spheroidal shape. Moreover, the number of objects with circularized effective radius larger than 1.5 kpc declines very fast.

The apparent g-band magnitude of the UDGs in our cluster area is 20.5<g<22.5 mag. This implies absolute magnitudes of -16$\lesssim M_g \lesssim$-14 mag. To put our UDGs in context with the rest of the galaxies in the Abell 168 area, we show in Fig. 4 the size versus absolute g-band magnitude plot for all the galaxies in the field of view at the redshift of the cluster. Galaxies with spectroscopic redshifts are shown with blue stars. We also include galaxies with photometric redshifts (purple dots) using the catalogue from Reis et al. (2012). A galaxy with photometric redshift is plotted if its redshift is compatible with being at the redshift of the cluster. We select those that are less than 3σ (with σ the photometric redshift error) away from z=0.045 and with a photometric redshift value of z<0.15. For the UDGs in our sample is not reasonable to use the photometric redshift from Reis et al. (2012). The reason is that the UDGs are significantly fainter (in terms of surface brightness)

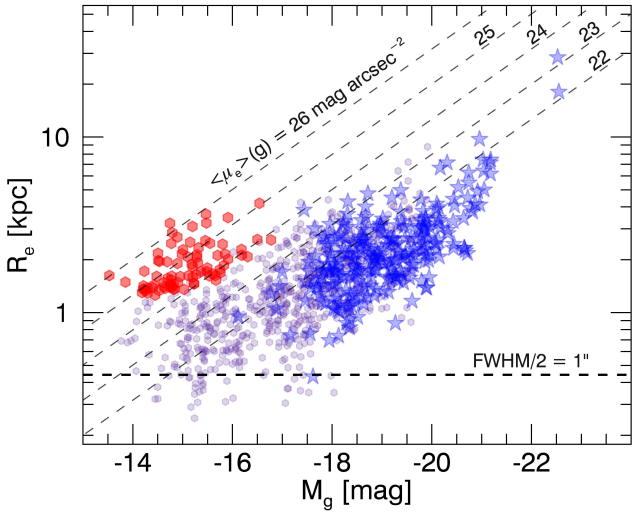

Figure 4. Circularized effective radius versus absolute g-band magnitude for all the galaxies in the Abell 168 area compatible with being at the cluster redshift. The structural parameters were derived using IMFIT (Erwin 2015). Galaxies with spectroscopic redshifts are shown with blue stars, whereas galaxies with photometric redshifts are shown with purple dots. The UDGs are plotted with red hexagons. The approximate value for the seeing FHWM of the images is 1 arcsec. In the figure we plot with an horizontal dashed line the value of FWHM/2 which is equivalent to 0.45 kpc at the redshift of the cluster. The inclined dashed lines indicate equal average surface brightness.

than the more compact galaxies at the same absolute magnitude. This produces an unacceptable uncertainty of their photometric redshifts.

As it has been found previously (see e.g. Koda et al. 2015; Muñoz et al. 2015), Fig. 4 shows that there is a region where galax-

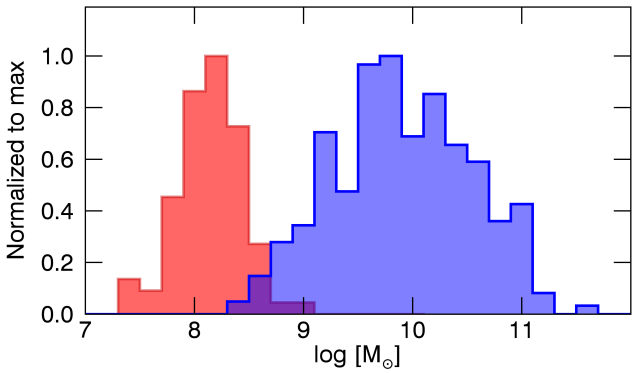

Figure 5. Stellar mass distribution of the galaxies in our sample. The red histogram shows the mass distribution of the UDGs whereas the blue histogram shows the distribution of galaxies with spectroscopic redshift 0.037<z<0.052. The histograms have been normalized to peak at 1.

ies considered as "normal" dwarfs and UDGs overlap. This is related to the criteria used for selecting UDGs which uses the central surface brightness (a quantity that it is not directly measured but extrapolated from the Sérsic fit to the surface brightness distribution of the galaxies). The apparent relation between the size of the UDGs and their absolute magnitude (found here and in previous works) is an artifact produced by the limiting surface brightness of the surveys.

Finally, we quantify the stellar mass distribution of our UDG galaxies. To do this we take advantage of our colour measurements. In particular, we use g-r to determine the mass-to-light ratio in r-band $(M/L)_r$. We follow the recipe by Bell et al. (2003). We have used a Kroupa (2001) Initial Mass Function (IMF). The stellar mass distribution of our galaxies is shown in Fig. 5, with peak around 10^8 $M_\odot$, similar to previous works using surveys with similar depths (see e.g. van der Burg et al. 2016). As a comparison we show the stellar mass distribution of the galaxies with spectroscopic redshifts 0.037<z<0.052.

5 SPATIAL DISTRIBUTION OF UDGS IN THE LARGE SCALE STRUCTURE

The goal of this paper is to explore how UDGs are spatially distributed in a large variety of environments. Once the final sample of UDGs is selected, we can probe whether they preferentially inhabit a particular region of the complex structure surrounding the Abell Cluster 168. We show the spatial distribution of the UDGs and the galaxies with spectroscopic redshifts compatible with being at the cluster distance in Fig. 6. The size of the area shown is limited by the declination width of the Stripe 82 survey (2.5°). In the R.A. direction we have expanded the area shown by 0.25°on each side to illustrate how the large scale structure in that direction continues. This is indicated with a darker blue colour. The blue stars are the galaxies with spectroscopic redshifts at 0.037<z<0.052. Large blue stars correspond to the dominant galaxies in each prominent substructure: UGC00797 (R.A.=18.73996, Dec.=0.43081, z=0.04482), UGC00842 (R.A.=19.72338, Dec.=-1.00199, z=0.04526) and UGC00753 (R.A.=18.01924, Dec.=-0.24512, z=0.04420). Red dots are the UDGs. To enhance the visibility of the large scale structure in Fig. 6 we have estimated the density distribution of the galaxies with spectroscopic redshifts at 0.037<z<0.052 using a bin size of 0.1°×0.1°. Then, we have smoothed the histogram for ease of visualization.

The most prominent structure, located a little above the central part of the plot is the Abell Cluster 168. This cluster is not fully relaxed, with an overdensity of galaxies slightly offset from the position of the main galaxy UGC00797 (Yang et al. 2004). The whole central structure has a radius of ~1.5 Mpc. The two other most conspicuous structures are the fossil group centered around the galaxy UGC00842 (Lopes de Oliveira et al. 2010) (bottom left corner of the figure) and the group around UGC00753. There are other filamentary-like structures, also a big empty region in the bottom right part of the image. The most remarkable result is that UDGs trace the large scale structure of spectroscopic galaxies.

5.1 The effect of interlopers in the spatial distribution of UDGs

Our selection criteria (colours, size and surface brightness) is constructed attempting to select all the UDGs at the redshift of the Abell 168 cluster. We try to avoid as much as possible contaminating sources projected in the line of sight. For instance, modeling different stellar population tracks (Vazdekis et al. 2015) in our colour-colour map, we find that at z>0.2, the vast majority of these models do not follow our colour-colour selection criteria. Additionally, our selection criteria (r_e >1.5 kpc at z=0.045) is equivalent to select objects with r_e >1.7 arcsec. This value corresponds to the following physical sizes at different redshifts: 3.1 kpc (z=0.1), 5.6 kpc (z=0.2) and 7.6 kpc (z=0.3). Considering that our typical UDG has g=21.5 mag, the absolute g-band restframe (K-corrected) at different redshifts will be: -16.7 mag (z=0.1), -18.3 mag (z=0.2) and -19.2 mag (z=0.3). Following Fig. 4, it can be easily seen that galaxies with the above absolute magnitudes and sizes are not expected to exist. In other words, if they exist, they are not common and consequently, their importance as a source of contamination is expected to be very small. These numbers illustrate that the probability of having in our catalogue of UDGs interlopers with z>0.1 is very low. For that reason, on what follows, we will concentrate on potential interlopers located in our line of sight up to z=0.1.

To evaluate the number of potential interlopers within our catalogue of UDGs, we explore the following idea: we quantify whether a given UDG is more likely to belong to our large scale structure (at z=0.045), or whether is more likely to be located in another large scale structure found in the same field up to z=0.1. To conduct this task, we assume that the likelihood of a given UDG candidate of belonging to a given structure is proportional to the number of galaxies with a given spectroscopic redshift in its neighborhood compatible with being part of that structure. On doing this, we are making the following assumption: UDGs are more abundant in the densest environments. This hypothesis is based on the findings by van der Burg et al. (2016) and Román & Trujillo (2016). These authors find a tight correlation between the number of UDGs and the mass of the host structure where they are embedded. This correlation has the following form: $N_{UDGs} \propto M^{\alpha}_{Host}$ with α ~1. Based on this, we estimate the probability of a given UDG in our list to pertain to a given structure as follows:

$$P(UDG(z)) \propto \sum_{i=1}^{N} M_i(z, M_\star > 2\times10^{10} M_\odot, R < 0.5 Mpc) \quad (1)$$

In other words, we sum the stellar mass of all the galaxies at a given (spectroscopic) redshift around our UDG candidate with $M_\star$>$2\times10^{10}$$M_\odot$ and within a projected radial distance R<0.5 Mpc. The reason why we select only spectroscopic galaxies with

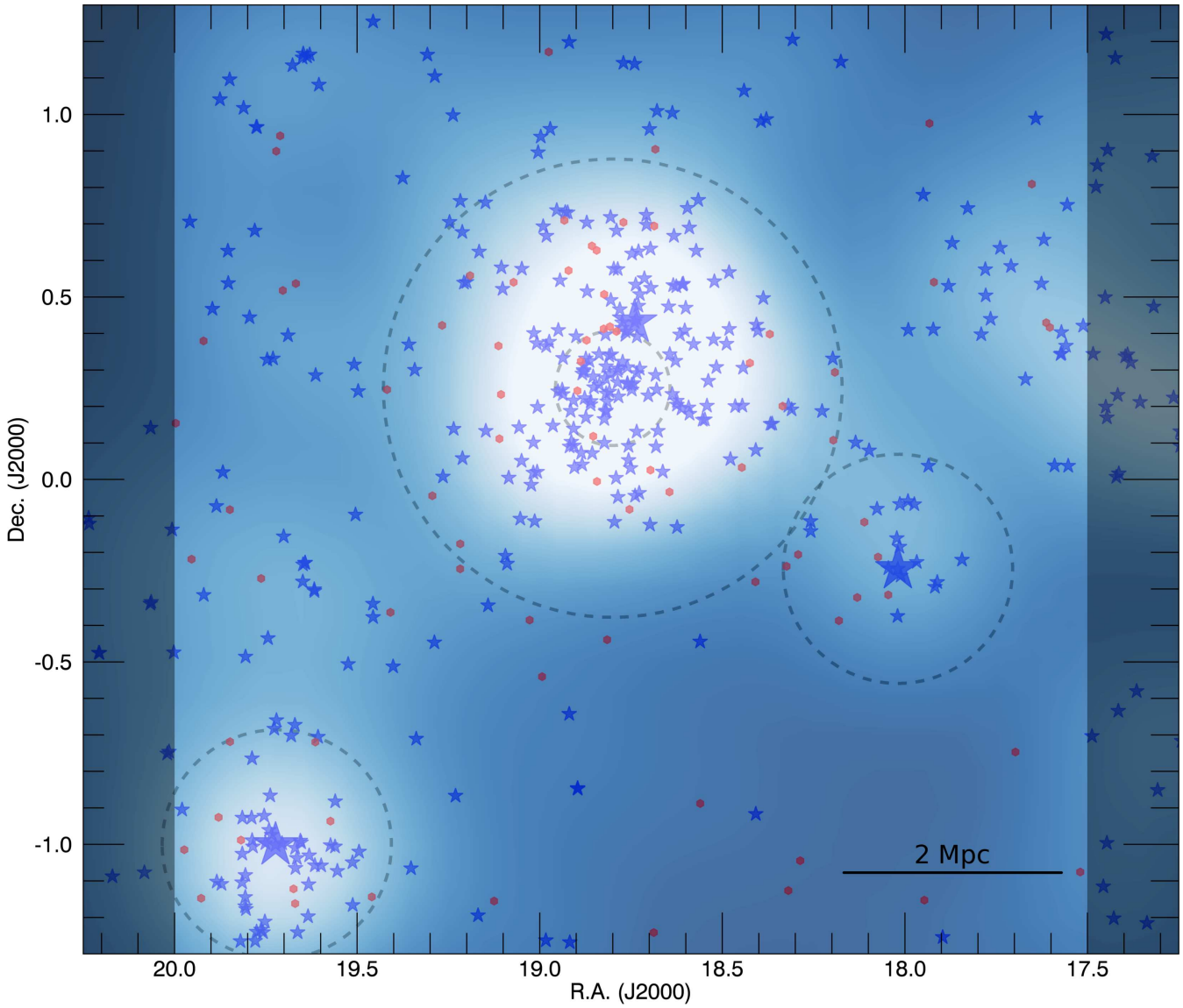

Figure 6. Spatial distribution of UDGs in the Abell cluster 168 and its surrounding large scale structure. The blue stars are the galaxies with spectroscopic redshifts at 0.037<z<0.052. Large blue stars correspond to the dominant galaxies in each substructure: UGC00797 (R.A.=18.73996, Dec.=0.43081, z=0.04482), UGC00842 (R.A.=19.72338 Dec.=-1.00199, z=0.04526) and UGC00753 (R.A.=18.01924 Dec.=-0.24512, z=0.04420). Red dots are the UDGs. The white areas correspond to the density distribution of the galaxies with spectroscopic redshifts. The gray dashed circles enclose the different zones explored in this paper: the cluster core (R<0.5 Mpc) and its outskirts (0.5<R<2 Mpc), the groups (R<1 Mpc) around UGC00753 and UGC00842, and filaments (remaining area). The horizontal bar indicates the equivalent size of 2 Mpc at the cluster distance.

$M_\star > 2\times10^{10} M_\odot$ is because this is the completeness stellar mass limit for galaxies up to z=0.1 in our SDSS spectroscopic sample (see Fig. 4 in Cebrián & Trujillo 2014). We are also assuming that the total stellar mass contained in the most massive galaxies is a proxy of the total mass of the structure where the UDG candidate is located.

To measure the above probability for each UDG candidate, we select different redshift slices following the distribution of the galaxies with spectroscopic redshift in our sample (see Fig. 7). Once we have estimated the probability for each of our UDG candidates, we sum the probability of the whole sample and we create the probability distribution of our sample of UDGs to belong to the different large scale structures within our field of view up to z=0.1. The result of this analysis is shown in the second row of Fig. 7. This figure shows that 69% of our UDG candidates are more likely to be located at the large scale structure at the redshift of the cluster (i.e. z=0.045). Naturally, the probability is not the same depending whether the UDG candidate is located. For this reason, we have repeated this exercise for different subsamples of our UDG galaxies accounting for their position within our field of view. For the UDGs located in the cluster's core (i.e. in the inner R<0.5 Mpc), the probability of pertaining to the cluster itself is 99% (in other words, the contamination in this region is negligible). For the region located in the outskirts of the cluster (0.5<R<2 Mpc) the probability of UDGs being placed there is 62%. Finally, for the galaxies well outside the cluster the probability of being located there is 46%. It is worth noting that our method is biased against potential UDGs located in the lowest density environments. So, our results, particularly in the

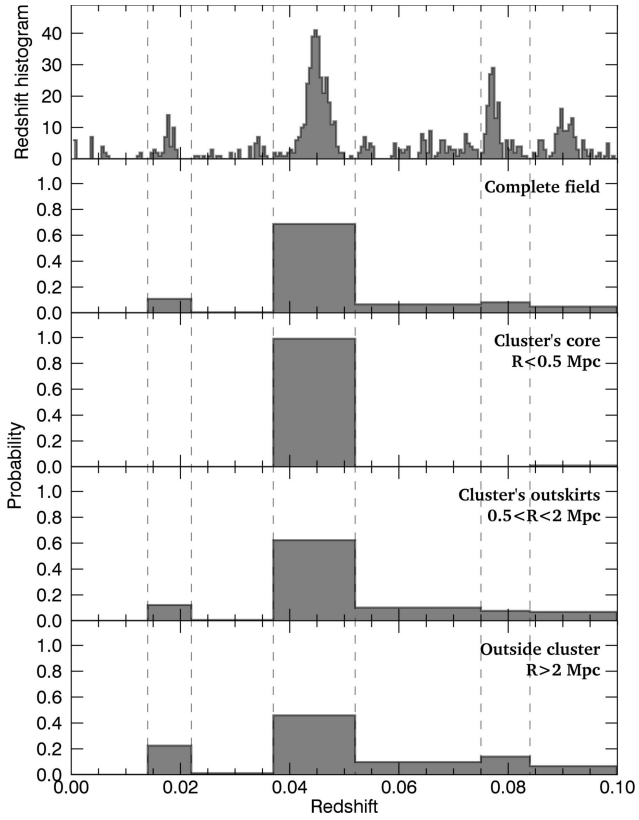

Figure 7. Redshift distribution and probability of UDGs to belong to the different large scale structure within our field of view up to z=0.1. The redshift distribution is shown in the upper panel. The rest of the panels show the probability of the UDGs to be located at a given redshift depending on their position within the field of view.

regions beyond the cluster's core are likely to be lower limits of the correct value.

Based on the above analysis we can estimate what would be the final number of UDGs in the different structures at z=0.045. For the cluster's core we will have (after removing the contamination): 5 UDGs, for the cluster's outskirts 17 UDGs and for the large scale structure surrounding the cluster 22 UDGs. This translates into the following percentage of UDG galaxies depending on the structure where they are located: 11±5% (cluster's core), 39±9% (cluster's outskirts) and 50±11% (outside the cluster).

6 THE ENVIRONMENT OF UDGS

We characterize the environment around each UDG by determining the average distance to its first five neighbours with stellar masses $>10^{9.5}$ $M_\odot$: $<r_5>$. The mass limit is chosen motivated by the stellar mass distribution shape of the galaxies with spectroscopy in Fig. 5, which suggests that the spectroscopic sample is complete at z=0.045 for stellar masses above this value. In addition, we take the average distance to the closest 5 neighbors to have a robust estimation (i.e. not strongly affected by shot noise) of the typical distance to the surrounding galaxies. We assume that both UDGs and galaxies with spectroscopic redshifts are all at the same comoving radial distance (i.e. z=0.045). The result of our analysis is shown in Fig. 8. For comparison, we also show the local density distribution of all the galaxies with spectroscopic redshifts in the cluster (i.e. also

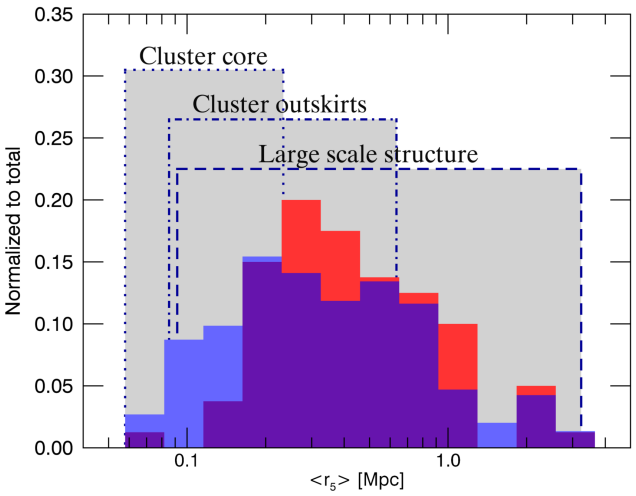

Figure 8. Average distance of the galaxies to their first five neighbors $< r_5 >$, a proxy for local density (see text for details). The histogram showing the average local density of UDGs is plotted in red. The blue histogram shows the same information for galaxies with spectroscopic redshifts 0.037<z<0.052 in the cluster field.

including the ones with $<10^{9.5}$ $M_\odot$) and its surrounding large scale structure. To contextualize the meaning of our local densities, we also show with vertical lines the range in density found for spectroscopic galaxies placed in the core of the Abell Cluster 168, in the cluster outskirts and in the large scale structure that surrounds it.

According to Fig. 8, UDGs tend to be located at lower environmental density than massive galaxies. The number densities of UDGs in each of the structures are (after removing contamination): 6±3 Mpc^{-2} in the cluster core, 1.4±0.4 Mpc^{-2} in the cluster outskirts and 0.4±0.1 Mpc^{-2} in the large scale structure. The contribution in stellar mass of the UDGs to the total stellar mass above 3×10^9 $M_\odot$ in each substructure are: ~0.06% in the cluster core, ~0.08% in the outskirt of the cluster and ~0.10% in the external large scale structure. The contribution of UDGs to the total stellar mass in the cluster is ~0.10%, a number similar (within a factor of 2) to the one reported by van der Burg et al. (2016), 0.2%. In the next section, we explore whether the environment of the galaxies affects their structural and colour properties. Exploring this is key to disentangling the origin and evolution of UDGs.

6.1 Structural properties of UDGs as a function of their environment

If UDGs are progressively infalling to the cluster center, it would be expected that during such a process their structural properties could be modified until they become disrupted (Yozin & Bekki 2015). We explore whether there is any hint of such a transformational process in our UDGs. Fig. 9 shows the structural properties of the UDGs and the rest of the galaxies with spectroscopic redshifts in our sample versus their local density.

To explore any trend between the structural parameters and local density, we separate our sample of UDGs in two groups with similar number of galaxies: those with $< r_5 >$ <0.45 Mpc and those with $< r_5 >$ >0.45 Mpc. In Table 1 we show the results of this exercise. We find a dependence on the structural properties of our UDGs sample as a function of the environment. We find a decrease of the stellar mass (by a factor of ~1.5), a decrease of the radius (by a mean of 0.23 kpc), fainter average surface brightness (~0.4 mag

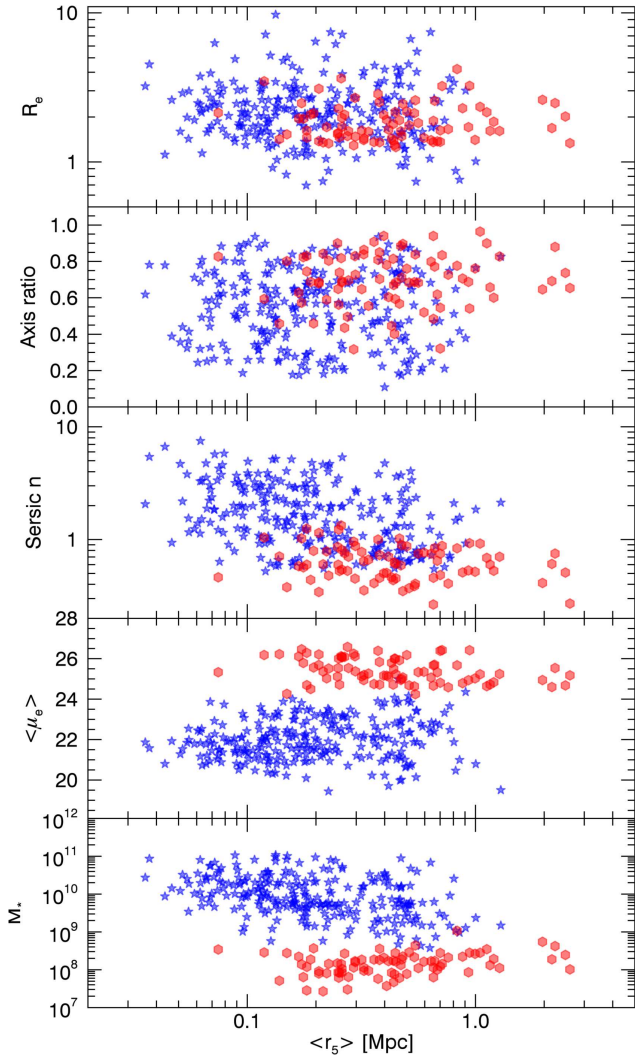

Figure 9. Structural properties of the galaxies in our sample (in the g-band) versus the average distance of the galaxies to their closest 5 neighbors with spectroscopic redshift $< r_5 >$ (a proxy for the local density). In red, the distribution of the UDGs, in blue the galaxies with spectroscopic redshifts 0.037<z<0.052.

Table 1. Average properties of the UDGs as function of their local density $< r_5 >$.

		$< r_5 > < 0.45$ Mpc	$< r_5 > > 0.45$ Mpc
$< g-r >$		0.47±0.02	0.47±0.02
$< r-i >$		0.19±0.02	0.18±0.02
$< n >$		0.67±0.04	0.62±0.04
$< r_e >$	(kpc)	1.71±0.06	1.94±0.09
$< \mu_e >$	(mag/arcsec^2)	25.6±0.1	25.2±0.1
$< b/a >$		0.69±0.02	0.71±0.02
$< M_\star >$	($\times 10^8 M_\odot$)	1.3±0.1	1.9±0.2

arcsec^{-2}), a larger Sérsic index n (a factor of ∼1.1) and a marginal lower axis ratio. These numbers are not corrected by the effect of contaminants as we assume the interlopers will not modify the average properties of our subsamples.

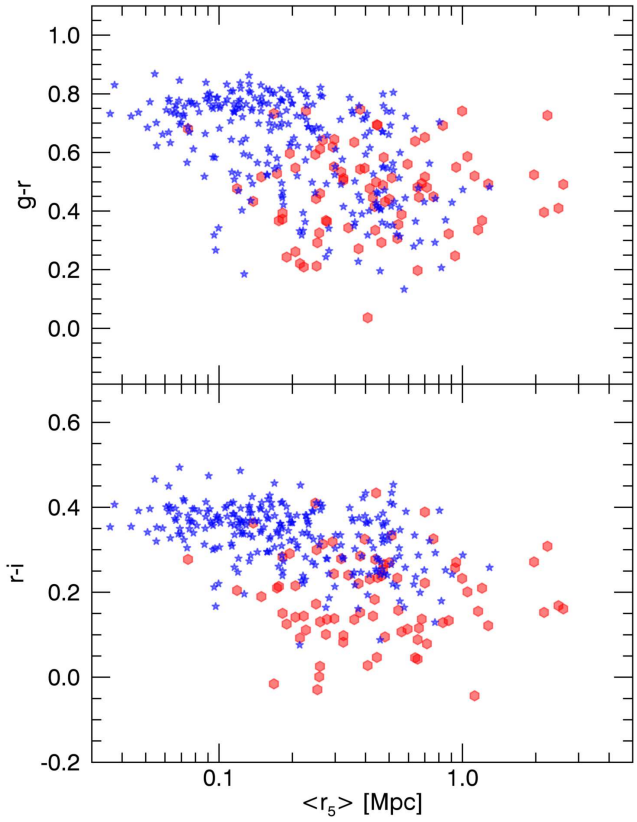

Figure 10. Colour versus the average distance of our galaxies to their closest 5 neighbors with spectroscopic redshift $< r_5 >$ (a proxy for the local density). In red, the distribution of the UDGs, in blue the galaxies with spectroscopic redshifts 0.037<z<0.052.

6.2 Colour of UDGs as a function of their environment

In this section, we explore whether the colour distribution of the UDGs depends on the environment where they reside. van Dokkum et al. (2015) find an average colour of <g-i>=0.8±0.1, while we find here 0.66±0.02 (r.m.s.=0.20). According to van Dokkum et al. (2015), this colour can be either reproduced by a stellar population with 7 Gyr and [Fe/H]=-1.4 or a population with 4 Gyr and [Fe/H]=-0.8. In both cases, this corresponds to galaxies significantly younger than the most massive galaxies of the cluster. Similarly, van der Burg et al. (2016) find a typical colour of g-r=0.6 (we find <g-r>=0.47±0.02 with r.m.s.=0.15) which implies an age of 2 Gyr assuming solar metallicity or 6 Gyr with [Fe/H]=-0.7. Our average colour values are compatible also with relatively modest ages: 3 Gyr ([Fe/H]=-1.3) or 2 Gyr ([Fe/H]=-1.7) (Vazdekis et al. 2015). It is worth noting that if we had not corrected the contaminants by their position in the colour-colour map, the average UDGs colours would be slightly redder: <g-r>=0.55±0.02 and <r-i>=0.25±0.02.

We can now take a look to the colour distribution of the UDGs as a function to their local density as characterized by the average distance to their 5 closest neighbors $< r_5 >$ (see Fig. 10). According to that Figure, the colours of UDGs are independent of their local density. We have repeated the same analysis done for the structural parameters to quantify this statement (see Table 1). Another interesting aspect is that UDGs are significantly bluer (∼0.3 mag in g-r and ∼0.2 in r-i) than the massive galaxies located in the densest region of the large scale structure. The vast majority of the UDGs

have colours consistent with the dwarf galaxies in the large scale structure at the cluster distance.

7 UDGS AND DWARF GALAXIES

The global distribution of the UDGs in the large scale structure, shown in Fig. 6, as well as the relationship between their colour and local density are suggestive of a scenario where UDGs are not significantly different, as a population, from dwarf galaxies with stellar masses around 10^9 $M_\odot$ (i.e. similar to LMC). In fact, we have explored whether the colours and spatial distribution of UDGs are similar to the dwarf ($1<M_\star<3\times10^9 M_\odot$) galaxies with spectroscopic redshift in our area[4]. For these galaxies we find the following colours: <g-r>=0.48±0.02 and <r-i>=0.25±0.01, very similar to the colours we get for the UDGs. Their spatial distribution is also compatible to the UDGs. We find 9±5% in the cluster core region, 34±9% in the outskirts of the cluster and 57±8% in the large scale structure. Doing exactly the same analysis but for galaxies with $\sim5\times10^{10} M_\odot$ (i.e. Milky-Way like objects), we find: <g-r>=0.79±0.02 and <r-i>=0.38±0.01 and the following number densities: 25±6% in the cluster core region, 37±7% in the outskirt of the cluster and 38±6% in the large scale structure. In other words, $L_\star$ galaxies are much redder than UDGs and are also spatially distributed very differently. The similar colour and spatial distribution of UDGs with dwarf galaxies and their discrepancy with more massive galaxies seems to favour an scenario where UDGs are more likely bona fide dwarfs than failed $L_\star$. We expand on this idea in the Discussion section.

8 DISCUSSION

Within the standard galaxy formation scheme, very diffuse galaxies are expected to form in initial fluctuations with low density (Fall & Efstathiou 1980; Mo et al. 1998) with blue colours, a large amount of gas and disk-like shapes (McGaugh & Bothun 1994). Moreover, these objects are not supposed to exist in high-density environments as the effect of tides will easily disrupt them (Dekel & Silk 1986; Rosenbaum et al. 2009; Galaz et al. 2011). However, UDGs are numerous in clusters, and the more massive the cluster, the more abundantly they can be found (e.g. van der Burg et al. 2016; Román & Trujillo 2016). There are two possible scenarios to explain these findings:

- First scenario. UDGs are a population connected to the cluster environment and they are born and survive in these dense regions since they are embedded in very massive (Milky-Way like) dark matter halos. Only in the very inner regions of the clusters they will be disrupted due to tidal effects. They should be common, however, in the outer regions of clusters.
- Second scenario. UDGs are regular dwarf galaxies that have been formed in the lowest density regions of the large scale structure. They have dark matter halos typical of dwarf galaxies. This means that, if they are accreted to cluster and/or group central regions, they can survive within them, but farther away from the densest regions compared to scenario one. Once they reach the peripheral regions of the densest structures, unless they have a radial orbit towards the central regions, they can survive for a long time in the outer parts as they are weakly influenced by dynamical friction (Smith et al. 2010, 2015).

Let's explore whether the current observational evidences support either of the above scenarios. The strongest observational evidence disfavoring that UDGs are failed $L_\star$ galaxies is the one by Beasley et al. (2016). These authors find that VCC1287, an UDG in the Virgo Cluster, has a dark matter halo of $\sim8\times10^{10}$ $M_\odot$. This is more than a factor of 10 smaller than the ones expected for $L_\star$ galaxies ($\gtrsim 10^{12}$ $M_\odot$). However, this result is just based on one single galaxy and VCC1287 is a particularly low mass ($\sim3\times10^7$ $M_\odot$) UDG (i.e. a factor of ∼3 less massive than most of the UDG population explored so far $\sim10^8$ $M_\odot$). Assuming that in this range of masses, M_{halo} will scale proportionality to $M_\star$, the Beasley et al. (2016) result will still disfavor the idea that UDGs with $M_\star$ $\sim10^8$ $M_\odot$ are failed $L_\star$ galaxies. This is because the mass of its dark matter halo would still be too low by a factor of 3. It is clear then that we need urgently to estimate the dark matter masses of more UDGs[5]. In the meantime, we can evaluate the outcomes of the other observational results.

A good test to support or disfavor any of the above scenarios is to explore the spatial distribution of UDGs. This test is based on the following two assumptions: a) the sizes of galaxies are a direct manifestation of the spin parameter of its halo (Mo et al. 1998) and b) the spin distribution is not strongly dependent on environment (Amorisco & Loeb 2016). Based on assumption number one, it follows that UDGs can be either regular dwarfs with high-spin halos or $L_\star$ galaxies with average spin halos. According to the assumption number two, the spatial distribution of UDGs will resemble those of the dark matter haloes where they are embedded. Consequently, we have explored in this paper which spatial distribution UDGs resemble most: $L_\star$ galaxies or those of regular dwarfs? In previous sections, we show that UDGs share the same spatial distributions and colours than regular dwarf galaxies with stellar mass 10^9 $M_\odot$, while they disagree with the distribution of more massive ($L_\star$ like) objects. Consequently, this could suggest that we can make the association that UDGs are more likely dwarf galaxies than failed $L_\star$ objects.

Following a similar argument, Amorisco & Loeb (2016) make the prediction: "Under the assumption that the spin distribution is not strongly dependent on environment and that these extended disks are capable of forming stars in a similar way when in isolation, our model suggests that an abundant tail of extended galaxies should be ubiquitous in both clusters and in the field". This is in fact what we see in this paper: UDGs are not a phenomenon exclusively linked to clusters of galaxies. Note that previously reported UDGs (with the exception of DGSAT I by Martínez-Delgado et al. 2016) have been found in dense (i.e. cluster environments). However, we find that UDGs are common outside the clusters, being clearly lo-

[4] Ideally, we would like to perform this analysis with dwarf galaxies with lower masses, i.e. closer to the UDGs masses, however, the very small number of spectroscopic objects with such low mass prevents us from conducting this task. For this reason, we made the compromise of exploring the spatial distribution of 10^9 $M_\odot$ dwarfs.

[5] Recently, Peng & Lim (2016) and Beasley & Trujillo (2016) using the number of globular clusters as a proxy for the dark matter halo mass of the galaxy, also find that the UDG DF17 inhabits a dark matter halo with $\sim10^{11}$ $M_\odot$, van Dokkum et al. (2016) found $\sim10^{12}$ $M_\odot$ for the DF44 UDG and Amorisco et al. (2016) analyzing HST imaging of 54 UDG in the Coma Cluster found low-mass haloes for this set of UDGs.

cated around groups and with hints of existence in the less dense structure in our field.

Both UDGs and $L_\star$ galaxies are found with the same proportion (∼38%) in the outskirts of the Abell Cluster 168. However, they strongly differ in the inner core region of the cluster (25% $L_\star$ vs 11% UDGs) as well as outside clusters (38% $L_\star$ vs 50% UDGs). This again supports the idea that UDGs are not failed $L_\star$ galaxies as they are scarce in the regions where the tides are strong on these objects. If they were sharing the same type of dark matter halos they should better withstand the harsh conditions of the cluster's core.

A final question we want to address is the following: Do we have any evidence favoring the formation of UDGs outside clusters and being later on accreted to the cluster periphery? If this were the case, this would be another hint that the second proposed scenario is more likely than the first one. Clusters of galaxies are very active locations within the large scale structure of the Universe, with significant continuous accretion of other galaxies by infall of minor substructures happening with high frequency (e.g. Fakhouri et al. 2010). For this reason, UDGs formed outside Abell 168 have to infall to the cluster at some point. This being the case, both the structural and colour properties of UDGs should reflect a gradual change in their values as we approach to the densest regions. Yozin & Bekki (2015) suggest that UDGs undergoing tidal fields should show a decrease on their stellar mass, a flattening of their structure (i.e. a decrease of their axis ratio) and a decline in their surface brightness. According to Fig. 9 and Table 1 there are a lower stellar mass (by a factor of ∼1.5), a decrease of radius (by a mean of 0.23 kpc), fainter average surface brightness (∼0.4 mag arcsec^{-2}), a larger Sérsic index n (a factor of ∼1.1) and a marginal lower axis ratio of the UDGs located in the densest regions compared to the galaxies in most isolated places. Similarly, Amorisco & Loeb (2016) predicts: "It can be expected that the isolated counterparts of cluster UDGs should have more clearly disky morphologies, and not appear as red and quenched". In this work, we do not find any clear hint neither in colour nor in axis ratio to support this conclusion[6]. Summarizing, while the structural properties of our galaxies show a qualitative agreement with the ideas of UDGs transformation while infalling into the cluster environment, we do not find any obvious relation between the colour of the UDGs as a function their local density. In particular, there is no obvious trend towards redder colours (i.e. older ages) in the central region of both the cluster and the largest groups. Nonetheless, recent work by (Román & Trujillo 2016; Di Cintio et al. 2016; Merritt et al. 2016) suggest that UDG can exist in the field, favoring the approach and results of this work, i.e. the dwarf nature of the UDGs.

9 SUMMARY

In this paper we have explored the properties of UDGs inhabiting the Abell Cluster 168 (z=0.045) and its rich surrounding large scale structure. This work represents an important step forward in understanding in which environments UDGs are born and it allows us to address in more detail the ultimate nature of the UDGs. For instance, among others scenarios: are UDGs regular dwarf galaxies inhabiting high-spin halos or are they failed $L_\star$ galaxies? The main conclusions of this observational work can be summarized as follows:

- UDGs are found over the whole scale structure defined by the Abell cluster 168 and its surroundings. Our data allow us to confirm the existence of UDGs in the Abell cluster 168 and groups present in our field, showing hints of the presence of UDGs in the filamentary structure. They are distributed (after removal of potential interlopers) as follows: 11±5% in the cluster's core, 39±9% in the outskirts of the cluster and 50±11% in the large scale structure around the cluster. The number densities of UDGs in each of the substructures are: 6±3 Mpc^{-2} in the cluster core, 1.4±0.4 Mpc^{-2} in the cluster outskirts and 0.4±0.1 Mpc^{-2} in the large scale structure.
- The spatial distribution of the UDGs is similar to that found for regular (∼10^9 $M_\odot$) dwarf galaxies but significantly different from that of $L_\star$ objects. Under the assumption that the spin distribution is not strongly dependent on the environment this can be understood as favoring the idea that UDGs are dwarf galaxies inhabiting high-spin halos (Amorisco & Loeb 2016).
- There is a gradual transformation of some of the structural properties of UDGs with the local density where they are located. From the lowest to the highest density we find: a decrease of the stellar mass (by a factor of ∼1.5), a decrease of the radius (by a mean of 0.23 kpc), fainter average surface brightness (∼0.4 mag arcsec^{-2}), a larger Sérsic index n (a factor of ∼1.1) and a marginal lower axis ratio. This transformation is in qualitative agreement with the idea that UDGs probably form outside the clusters and are later on accreted through the infall of groups and filaments towards the cluster's central regions where they are finally destroyed by disruption.
- We do not find a strong change in the colours of the UDGs with the local density. UDGs colours (<(g-r)>=0.47±0.02 and <(r-i)>=0.19±0.02) are compatible with the colours of dwarf galaxies. These values can be interpreted as typical of ages between 2 to 6 Gyr depending on the assumed metallicity. For extremely low metallicities, this age can rise up to ∼12 Gyr.

[6] It is worth noting that our selection criteria for selecting UDGs could be biased against disk-like galaxies for two reasons: it is based on circular R_e (i.e. it avoids selecting the most inclined galaxies) and it is based on central surface brightness (again that means that inclined projections are disfavored).

ACKNOWLEDGMENTS

We are grateful to the referee for his/her constructive comments. We want to specially thank Mike Beasley for his helpful comments during the development of this work. We thank Juergen Fliri for his careful work on The IAC Stripe 82 Legacy Project. Lee Kelvin is also acknowledged for his help. This research was supported by the Instituto de Astrofísica de Canarias. The authors of this paper acknowledges support from grant AYA2013-48226-C3-1-P from the Spanish Ministry of Economy and Competitiveness (MINECO). Javier Román thanks the Spanish Ministry of Economy and Competitiveness (MINECO) for financing his PhD through FPI grant.

REFERENCES

Amorisco, N. C., & Loeb, A. 2016, MNRAS, 459, L51
Amorisco, N. C., Monachesi, A., & White, S. D. M. 2016, arXiv:1610.01595
Beasley, M. A., Romanowsky, A. J., Pota, V., et al. 2016, ApJ, 819, L20
Beasley, M. A., & Trujillo, I. 2016, ApJ, 830, 23
Bertin E., Arnouts S., 1996, A&AS, 117, 393
Bertin E., Mellier Y., Radovich M., Missonnier G., Didelon P., Morin B., 2002, ASPC, 281, 228

Bell, Eric F.; McIntosh, Daniel H.; Katz, Neal; Weinberg, Martin D., 2003 ,ApJ,149,289B
Burkholder, V., Impey, C., & Sprayberry, D. 2001, AJ, 122, 2318
Bothun, G. D., Impey, C. D., & Malin, D. F. 1991, ApJ, 376, 404
Cebrián, M., & Trujillo, I. 2014, MNRAS, 444, 682
Chilingarian, Igor V.; Melchior, Anne-Laure; Zolotukhin, Ivan Yu. 2010, MNRAS, 405, 1409
Dalcanton, J. J., Spergel, D. N., Gunn, J. E., Schmidt, M., & Schneider, D. P. 1997, AJ, 114, 635
Dekel, A., & Silk, J. 1986, ApJ, 303, 39
Di Cintio, A., Brook, C. B., Dutton, A. A., et al. 2016, arXiv:1608.01327
Erwin, P. 2015, ApJ, 799, 226
Fakhouri, O., Ma, C.-P., & Boylan-Kolchin, M. 2010, MNRAS, 406, 2267
Fall, S. M., & Efstathiou, G. 1980, MNRAS, 193, 189
Fliri, J., & Trujillo, I. 2016, MNRAS, 456, 1359
Galaz, G., Herrera-Camus, R., Garcia-Lambas, D., & Padilla, N. 2011, ApJ, 728, 74
Impey, C., Bothun, G., & Malin, D. 1988, ApJ, 330, 634
Koda, J., Yagi, M., Yamanoi, H., & Komiyama, Y. 2015, ApJ, 807, L2
Kroupa, Pavel. 2001, MNRAS,322,231
Lopes de Oliveira, R.; Carrasco, E. R.; Mendes de Oliveira, C.; Bortoletto, D. R.; Cypriano, E.; Sodr, L., Jr.; Lima Neto, G. B. 2010, ApJ,139,L216
MacArthur, Lauren A. Courteau, Stphane & Holtzman, Jon A., 2003, ApJ, 582, 689
Martínez-Delgado, D., Läsker, R., Sharina, M., et al. 2016, AJ, 151, 96
McGaugh, S. S., & Bothun, G. D. 1994, AJ, 107, 530
Merritt, A., van Dokkum, P., Danieli, S., et al. 2016, arXiv:1610.01609
Mihos, J. C., Durrell, P. R., Ferrarese, L., et al. 2015, ApJ, 809, L21
Mo, H. J., Mao, S., & White, S. D. M. 1998, MNRAS, 295, 319
Muñoz, R. P., Eigenthaler, P., Puzia, T. H., et al. 2015, ApJ, 813, L15
Peng, E. W., & Lim, S. 2016, ApJ, 822, L31
Reis, Ribamar R. R. et al. 2012, 2012ApJ...747...59R
Román, J., & Trujillo, I. 2016, arXiv:1610.08980
Rosenbaum, S. D., Krusch, E., Bomans, D. J., & Dettmar, R.-J. 2009, A&A, 504, 807
Schlafly, E. F., & Finkbeiner, D. P. 2011, ApJ, 737, 103
Sersic, J. L. 1968, Cordoba, Argentina: Observatorio Astronomico, 1968
Smith, R., Davies, J. I., & Nelson, A. H. 2010, MNRAS, 405, 1723
Smith, R., Sánchez-Janssen, R., Beasley, M. A., et al. 2015, MNRAS, 454, 2502
van der Burg, Remco F. J., Muzzin, A., & Hoekstra, H. 2016, A&A, 590, A20
van Dokkum, P. G., Abraham, R., Merritt, A., et al. 2015, ApJ, 798, L45
van Dokkum, P. G.; Romanowsky, A. J.; Abraham, R.; Brodie, J. P.; Conroy, C.; Geha, M.; Merritt, A.; Villaume, A.; Zhang, J. 2015, ApJ, 804, L26
van Dokkum, P., Abraham, R., Brodie, J., et al. 2016, ApJ, 828, L6
Vazdekis, A., Coelho, P., Cassisi, S., et al. 2015, MNRAS, 449, 1177
Yang, Y., Zhou, X., Yuan, Q., et al. 2004, ApJ, 600, 141
Yozin, C., & Bekki, K. 2015, MNRAS, 452, 937

APPENDIX A: ROBUSTNESS OF THE STRUCTURAL PARAMETERS

In this section we compare the structural properties, apparent magnitude and effective radius provided by IMFIT and SExtractor for the whole set of galaxies in our field. This comparison is done for those objects that satisfy the SExtractor detection criteria and the primordial colour cut explained in Section 3. Our results are shown in Fig. A1.

There is a very good agreement in all the filters related to the global apparent magnitude of the objects. At the magnitude limit where most of the UDGs are (20.5<g<22.5 mag), the r.m.s. between SExtractor and IMFIT is around 0.1 mag. In relation to the effective radius along the semimajor axis, r_e, we find that there is a good 1:1 relation for those galaxies larger than the typical seeing

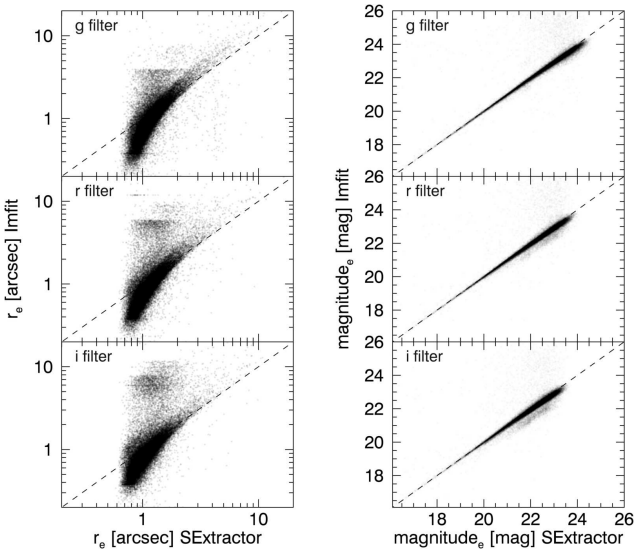

Figure A1. Size and apparent magnitude comparison between SExtractor and IMFIT for all the galaxies detected in the cluster field.

of the Stripe 82 data (∼1 arcsec). This is as expected, as SExtractor does not take into account the seeing of the data when estimating r_e. For this reason, their r_e is overestimated. The typical r_e of the UDGs in our image is ∼2 arcsec. At these values, the r.m.s. in the size estimation between both codes 10%.

In addition, we have checked the robustness of the structural parameters for our UDGs comparing the sizes and Sérsic indexes among the different filters used. The result of this comparison is shown in Fig. A2. We do find a nice agreement between these structural parameters independently of the filter used. As expected the effective radius along the semimajor axis r_e is estimated more precisely than the Sérsic index.

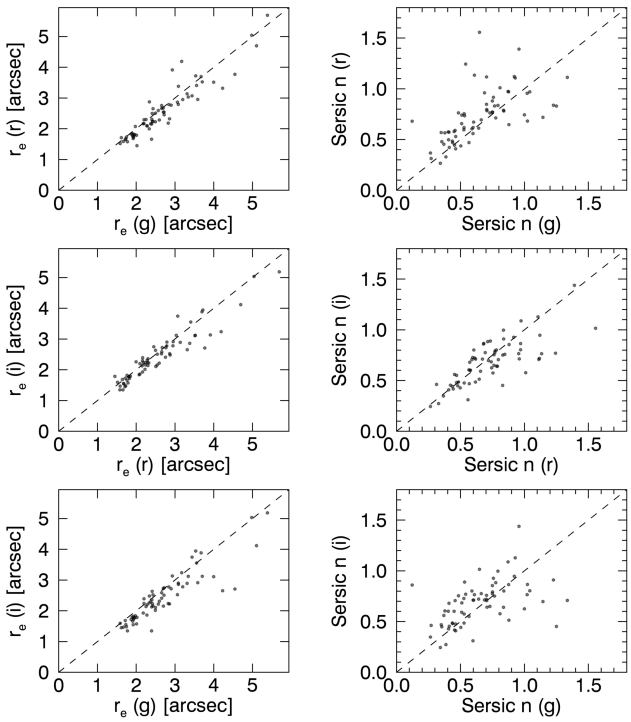

Figure A2. Robustness of the structural parameters r_e and n obtained with IMFIT for the set of UDGs explored in this work. The size and shape of the UDGs are compared between the different filters: g, r and i.

APPENDIX B: CATALOGUE OF UDGS

ID	R.A. (J2000)	Dec (J2000)	$\mu_g(0)$ mag arcsec^{-2}	r_e (kpc)	M_g (mag)	b/a	n
IAC01	19.9966	0.1540	$25.4^{+0.5}_{-0.5}$	4.4±0.4	-15.6±0.1	0.54±0.08	0.93±0.23
IAC02	19.9733	-1.0147	$25.3^{+0.5}_{-0.4}$	2.5±0.2	-14.6±0.1	0.76±0.11	0.87±0.22
IAC03	19.9533	-0.2186	$24.8^{+0.4}_{-0.3}$	1.7±0.2	-14.6±0.1	0.62±0.09	0.65±0.16
IAC04	19.9272	-1.1476	$24.4^{+0.4}_{-0.4}$	2.0±0.2	-15.2±0.1	0.65±0.10	0.78±0.19
IAC05	19.9205	0.3794	$24.4^{+0.3}_{-0.2}$	1.9±0.2	-15.6±0.1	0.73±0.11	0.41±0.10
IAC06	19.8794	-0.9259	$25.0^{+0.2}_{-0.2}$	1.5±0.2	-14.5±0.1	0.86±0.13	0.35±0.09
IAC07	19.8484	-0.0829	$24.6^{+0.2}_{-0.2}$	1.4±0.1	-14.8±0.1	0.94±0.14	0.27±0.07
IAC08	19.8480	-0.7186	$25.5^{+0.4}_{-0.3}$	2.1±0.2	-14.3±0.1	0.40±0.06	0.63±0.16
IAC09	19.8180	-0.9883	$24.1^{+0.2}_{-0.2}$	1.7±0.2	-15.7±0.1	0.80±0.12	0.38±0.09
IAC10	19.7629	-0.2714	$24.8^{+0.3}_{-0.3}$	2.2±0.2	-15.3±0.1	0.78±0.12	0.51±0.13
IAC11	19.7214	0.8993	$24.9^{+0.2}_{-0.2}$	2.6±0.3	-15.8±0.1	0.90±0.13	0.35±0.09
IAC12	19.7106	0.9414	$24.5^{+0.4}_{-0.4}$	2.1±0.2	-15.3±0.1	0.60±0.09	0.70±0.18
IAC13	19.7034	0.5177	$24.4^{+0.4}_{-0.4}$	1.6±0.2	-14.7±0.1	0.80±0.12	0.75±0.19
IAC14	19.6741	-1.1219	$25.2^{+0.3}_{-0.2}$	1.5±0.1	-14.1±0.1	0.80±0.12	0.48±0.12
IAC15	19.6678	0.5367	$24.5^{+0.3}_{-0.2}$	2.2±0.2	-15.7±0.1	0.55±0.08	0.48±0.12
IAC16	19.6697	-1.1622	$25.7^{+0.3}_{-0.3}$	2.4±0.2	-14.6±0.1	0.68±0.10	0.54±0.14
IAC17	19.6144	-0.7196	$24.3^{+0.3}_{-0.3}$	1.7±0.2	-15.2±0.1	0.74±0.11	0.53±0.13
IAC18	19.5731	-0.9363	$25.8^{+0.3}_{-0.2}$	3.0±0.3	-15.0±0.1	0.83±0.12	0.45±0.11
IAC19	19.4598	-1.1439	$25.5^{+0.4}_{-0.3}$	2.8±0.3	-15.0±0.1	0.59±0.09	0.61±0.15
IAC20	19.4180	0.2460	$24.8^{+0.3}_{-0.3}$	2.1±0.2	-15.2±0.1	0.94±0.14	0.50±0.13
IAC21	19.4088	-0.3643	$24.0^{+0.3}_{-0.2}$	2.8±0.3	-16.8±0.1	0.84±0.13	0.40±0.10
IAC22	19.2940	-0.0448	$24.4^{+0.2}_{-0.2}$	2.6±0.3	-16.2±0.1	0.69±0.10	0.39±0.10
IAC23	19.2672	0.4220	$24.5^{+0.2}_{-0.2}$	2.1±0.2	-15.7±0.1	0.68±0.10	0.37±0.09
IAC24	19.2176	-0.1766	$24.6^{+0.4}_{-0.4}$	2.0±0.2	-14.9±0.1	0.52±0.08	0.77±0.19
IAC25	19.2178	-0.2451	$25.7^{+0.4}_{-0.4}$	2.4±0.2	-14.3±0.1	0.32±0.05	0.75±0.19
IAC26	19.1906	0.5585	$24.4^{+0.3}_{-0.2}$	1.6±0.2	-15.1±0.1	0.70±0.11	0.46±0.11
IAC27	19.1249	-1.1553	$24.4^{+0.3}_{-0.3}$	2.7±0.3	-16.1±0.1	0.71±0.11	0.51±0.13
IAC28	19.1129	0.3658	$25.5^{+0.3}_{-0.2}$	2.2±0.2	-14.6±0.1	0.45±0.07	0.46±0.12
IAC29	19.1103	0.1114	$24.4^{+0.4}_{-0.3}$	1.5±0.2	-14.7±0.1	0.84±0.13	0.64±0.16
IAC30	19.1059	0.2328	$24.4^{+0.3}_{-0.2}$	2.0±0.2	-15.5±0.1	0.81±0.12	0.44±0.11
IAC31	19.0715	0.5402	$25.2^{+0.4}_{-0.4}$	2.7±0.3	-15.1±0.1	0.85±0.13	0.73±0.18
IAC32	19.0276	-0.3854	$24.5^{+0.3}_{-0.3}$	2.1±0.2	-15.4±0.1	0.69±0.10	0.53±0.13
IAC33	18.9934	-0.5405	$24.6^{+0.4}_{-0.4}$	1.8±0.2	-14.8±0.1	0.83±0.12	0.70±0.18
IAC34	18.9753	1.1713	$25.4^{+0.3}_{-0.2}$	2.7±0.3	-15.2±0.1	0.48±0.07	0.46±0.11
IAC35	18.9325	0.7096	$24.2^{+0.3}_{-0.2}$	2.5±0.3	-16.3±0.1	0.69±0.10	0.44±0.11
IAC36	18.9211	0.5722	$25.3^{+0.6}_{-0.5}$	3.2±0.3	-14.9±0.1	0.81±0.12	1.00±0.25
IAC37	18.8968	0.2427	$25.0^{+0.6}_{-0.5}$	4.5±0.5	-15.8±0.1	0.59±0.09	1.04±0.26
IAC38	18.8872	0.3236	$25.0^{+0.3}_{-0.2}$	2.3±0.2	-15.3±0.1	0.83±0.12	0.46±0.12
IAC39	18.8716	0.3812	$24.8^{+0.6}_{-0.6}$	3.7±0.4	-15.4±0.1	0.69±0.10	1.14±0.29
IAC40	18.8571	0.6398	$24.5^{+0.5}_{-0.4}$	1.7±0.2	-14.6±0.1	0.73±0.11	0.88±0.22
IAC41	18.8534	0.1183	$25.3^{+0.6}_{-0.5}$	3.3±0.3	-14.9±0.1	0.57±0.09	1.02±0.26
IAC42	18.8441	0.6275	$25.4^{+0.4}_{-0.4}$	3.1±0.3	-15.2±0.1	0.44±0.07	0.76±0.19
IAC43	18.8432	-0.0056	$24.9^{+0.4}_{-0.3}$	1.5±0.1	-14.2±0.1	0.84±0.13	0.60±0.15
IAC44	18.8248	0.4125	$25.5^{+0.2}_{-0.2}$	1.7±0.2	-14.2±0.1	0.68±0.10	0.34±0.09
IAC45	18.8234	0.5071	$24.3^{+0.4}_{-0.4}$	2.2±0.2	-15.5±0.1	0.59±0.09	0.79±0.20
IAC46	18.8153	-0.4392	$24.2^{+0.3}_{-0.3}$	2.0±0.2	-15.5±0.1	0.66±0.10	0.60±0.15
IAC47	18.8077	0.4186	$25.3^{+0.3}_{-0.3}$	2.1±0.2	-14.6±0.1	0.82±0.12	0.57±0.14
IAC48	18.7897	0.4053	$25.6^{+0.4}_{-0.4}$	2.1±0.2	-14.1±0.1	0.46±0.07	0.71±0.18
IAC49	18.7707	0.7043	$24.2^{+0.3}_{-0.3}$	1.7±0.2	-15.2±0.1	0.74±0.11	0.60±0.15
IAC50	18.7542	-0.0821	$24.7^{+0.7}_{-0.6}$	1.8±0.2	-13.7±0.1	0.83±0.12	1.25±0.31
IAC51	18.6968	0.0255	$24.8^{+0.5}_{-0.4}$	3.1±0.3	-15.7±0.1	0.46±0.07	0.79±0.20
IAC52	18.6864	0.6942	$25.6^{+0.3}_{-0.3}$	2.5±0.2	-14.6±0.1	0.63±0.09	0.58±0.15
IAC53	18.6833	0.9045	$24.5^{+0.3}_{-0.3}$	1.7±0.2	-15.0±0.1	0.88±0.13	0.59±0.15
IAC54	18.6877	-1.2416	$24.7^{+0.3}_{-0.2}$	3.2±0.3	-16.4±0.1	0.65±0.10	0.41±0.10
IAC55	18.6447	-0.0344	$25.2^{+0.5}_{-0.5}$	2.3±0.2	-14.3±0.1	0.32±0.05	0.96±0.24
IAC56	18.5604	-0.8880	$24.8^{+0.4}_{-0.4}$	2.6±0.3	-15.3±0.1	0.88±0.13	0.75±0.19
IAC57	18.4465	0.0327	$25.5^{+0.1}_{-0.1}$	1.7±0.2	-14.4±0.1	0.67±0.10	0.12±0.03
IAC58	18.4244	0.3189	$24.5^{+0.7}_{-0.6}$	3.0±0.3	-15.2±0.1	0.56±0.08	1.23±0.31

IAC59	18.4093	-0.2806	$24.6^{+0.3}_{-0.3}$	1.6±0.2	-14.8±0.1	0.76±0.11	0.52±0.13
IAC60	18.3700	0.3980	$25.3^{+0.5}_{-0.4}$	2.1±0.2	-14.3±0.1	0.69±0.10	0.81±0.20
IAC61	18.3349	0.2009	$26.2^{+0.3}_{-0.3}$	2.1±0.2	-13.8±0.1	0.50±0.07	0.53±0.13
IAC62	18.3193	-1.1266	$25.1^{+0.2}_{-0.2}$	1.7±0.2	-14.7±0.1	0.65±0.10	0.27±0.07
IAC63	18.3238	-0.2380	$24.8^{+0.5}_{-0.4}$	4.8±0.5	-16.5±0.1	0.78±0.12	0.84±0.21
IAC64	18.2922	-0.2059	$25.5^{+0.5}_{-0.4}$	3.5±0.4	-15.1±0.1	0.83±0.13	0.88±0.22
IAC65	18.2867	-1.0447	$24.3^{+0.3}_{-0.3}$	2.3±0.2	-15.9±0.1	0.74±0.11	0.51±0.13
IAC66	18.1960	0.1074	$24.5^{+0.3}_{-0.2}$	1.4±0.1	-14.8±0.1	0.91±0.14	0.41±0.10
IAC67	18.1917	0.2934	$24.8^{+0.6}_{-0.5}$	2.5±0.3	-14.8±0.1	0.57±0.09	1.02±0.26
IAC68	18.1807	-0.3870	$24.8^{+0.5}_{-0.4}$	2.9±0.3	-15.4±0.1	0.77±0.12	0.84±0.21
IAC69	18.1305	-0.3235	$24.9^{+0.3}_{-0.2}$	1.5±0.2	-14.4±0.1	0.68±0.10	0.45±0.11
IAC70	18.1110	-0.1171	$24.7^{+0.4}_{-0.3}$	2.1±0.2	-15.1±0.1	0.56±0.08	0.66±0.17
IAC71	18.0735	-0.2127	$24.2^{+0.5}_{-0.4}$	1.6±0.2	-14.7±0.1	0.90±0.13	0.86±0.22
IAC72	18.0456	-0.3164	$24.4^{+0.7}_{-0.7}$	4.0±0.4	-15.7±0.1	0.82±0.12	1.34±0.33
IAC73	17.9467	-1.1528	$24.1^{+0.4}_{-0.3}$	2.0±0.2	-15.7±0.1	0.69±0.10	0.61±0.15
IAC74	17.9327	0.9754	$24.4^{+0.3}_{-0.3}$	2.4±0.2	-15.8±0.1	0.60±0.09	0.53±0.13
IAC75	17.9204	0.5405	$24.1^{+0.5}_{-0.5}$	1.8±0.2	-15.0±0.1	0.71±0.11	0.89±0.22
IAC76	17.6973	-0.7469	$24.2^{+0.5}_{-0.5}$	2.4±0.2	-15.4±0.1	0.96±0.14	0.92±0.23
IAC77	17.6523	0.8092	$24.6^{+0.4}_{-0.4}$	2.2±0.2	-15.1±0.1	0.68±0.10	0.75±0.19
IAC78	17.6129	0.4294	$24.9^{+0.4}_{-0.4}$	1.9±0.2	-14.6±0.1	0.70±0.10	0.70±0.18
IAC79	17.6030	0.4164	$25.0^{+0.3}_{-0.3}$	1.9±0.2	-14.7±0.1	0.65±0.10	0.60±0.15
IAC80	17.5198	-1.0757	$24.0^{+0.4}_{-0.3}$	2.3±0.2	-15.9±0.1	0.90±0.13	0.69±0.17

Table B1: Position and structural properties of the selected UDG candidates in the area surrounding Abell Cluster 168. The structural parameters were derived using IMFIT (Erwin 2015). In the table, the effective radius provided r_e is the value along the semimajor axis.